

Extended deep equatorial layering as a possible imprint of inertial instability

M. d'Orgeville,¹ B. L. Hua,¹ R. Schopp,¹ and L. Bunge²

Received 25 June 2004; accepted 7 October 2004; published 18 November 2004.

[1] The deep equatorial track of the world ocean is subject to intense zonal flow fields that still remain to be better understood. Inertial instability has been invoked to explain some of its features. Here we present possible in situ imprints of such a mechanism in the equatorial Atlantic Ocean below the thermocline. We analyse the observed pattern of homogeneous density layers of 50–100 m vertical scale, which are characterized by a large meridional coherency up to 2° of latitude, a concentration in the vicinity of the equator and foremost a vertical localization within regions of well-mixed angular momentum (westward jets). These distinctive properties suggest inertial instability to be a plausible mechanism for this extended layering. Numerical simulations forced by a time-oscillating shear reproduce the observed density layering characteristics. The prescription of deep jets in the background flow controls the vertical localization of the layering inside westward jets. **INDEX TERMS:** 4231 Oceanography: General: Equatorial oceanography; 4283 Oceanography: General: Water masses; 4568 Oceanography: Physical: Turbulence, diffusion, and mixing processes. **Citation:** d'Orgeville, M., B. L. Hua, R. Schopp, and L. Bunge (2004), Extended deep equatorial layering as a possible imprint of inertial instability, *Geophys. Res. Lett.*, 31, L22303, doi:10.1029/2004GL020845.

1. Introduction

[2] This study presents new observations of meridionally extended density layering within the deep equatorial Atlantic Ocean, at 50–100 m vertical scale. Similar density layerings have also been observed as temperature/salt intrusions in the equatorial Pacific surface layers [Richards and Banks, 2002], and as vertically homogeneous density layers in the equatorial Indian Ocean [Dengler and Quadfasel, 2002].

[3] In all equatorial oceans, the deep background flow corresponds to a vertically- and meridionally-complex zonal circulation, with alternate-signed jets of 400–800 m vertical scale [e.g., Bourlès et al., 2003, and references therein]. A distinguishing mark of such zonal circulation is the meridional homogenization of angular momentum within westward jets, as observed by Bourlès et al. [2003] and already noted for the deep equatorial Pacific by Hua et al.

[1997], who invoke inertial instability as the underlying homogenization mechanism.

[4] A first purpose of this paper is to demonstrate that the deep Atlantic layering is vertically localized within regions of meridionally homogeneous angular momentum, pointing out inertial instability as a plausible formation mechanism.

[5] In previous studies of inertial instability in the deep equatorial ocean, the shear source necessary for the existence of the instability remains to be identified unambiguously [Hua et al., 1997]. A steady classical shear flow [Dunkerton, 1981] cannot be invoked for the deep equatorial ocean since observed shears are often small and may not persist long enough to drive the instability [Send et al., 2002]. However, d'Orgeville and Hua [2004] show that a time-oscillating shear is able to trigger inertial instability, for smaller amplitude forcing than the classical steady case. They invoke the high-frequency variability which is ubiquitous in deep mooring arrays observation (e.g., L. Bunge et al., Variability of the horizontal velocity structure in the upper 1600 m of the water column on the equator at 10°W, submitted to *Journal of Physical Oceanography*, 2004, hereinafter referred to as Bunge et al., submitted manuscript, 2004) as a possible source of time-oscillating shears.

[6] A second purpose of this work, is to simulate numerically the 50–100 m density layering and to reproduce their vertical spatial localization within regions of meridionally homogeneous angular momentum. A new feature of the modelling is the inclusion of a time-oscillating shear of realistic amplitude to drive inertial instability.

2. Extended Deep Equatorial Layering

[7] A scrutiny of Atlantic equatorial density profiles reveals the existence of stair-like structures, with thin homogeneous density layers (Figure 1a) of typical 50–100 meters height. This phenomenon is best detected by sharp density jumps separating two layers. The jumps correspond to maxima in stratification strength, more precisely to maxima in squared Brunt-Väisälä frequency N^2 (Figure 1b), and are clearly distinguishable from the mean background stratification (dashed line). A latitudinal section of stratification anomaly $(N^2 - \langle N^2 \rangle) / \langle N^2 \rangle$ (e.g., at 23°W; Figure 2) (where $\langle \rangle$ corresponds to the latitudinal average of all profiles of the meridional section) highlights the importance of layering, concentrated within 1° to 2° of latitude around the equator and over the whole water column below the thermocline. We have checked both the ubiquity and similarity of the spatial characteristics of this layering in all available fine-scale meridional transects in the equatorial Atlantic Ocean (WOCE data set and EQUALANT campaigns). Dengler and Quadfasel [2002] observed similar

¹Laboratoire de Physique des Océans, Institut Français de Recherche pour l'Exploitation de la Mer, Plouzane, France.

²Laboratoire d'Océanographie Dynamique et de Climatologie, Institut de Recherche pour le Développement, Paris, France.

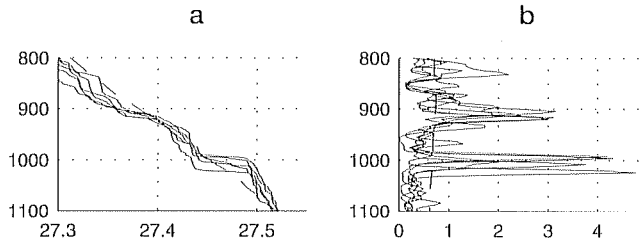


Figure 1. Vertical profiles of five adjacent stations between 0.6°S and 0.6°N at 10°W (EQUALANT 2000). (a) Potential density ($\text{kg}\cdot\text{m}^{-3}$). (b) N^2 (10^{-5}s^{-2}). Dashed lines in (a) and (b) correspond to meridional means, $\langle\rho\rangle$ and $\langle N^2\rangle$, of all profiles of the 10°W section (6°S – 3°N).

concentrations of stair-like structures in the central equatorial Indian Ocean, using individual CTD profiles.

[8] In the Atlantic case, Figure 1a shows that the signal can be moreover well correlated between meridionally adjacent CTD stations, advocating an extent up to 2° in latitude. Figure 1a reveals that a given step corresponds to a unique density interval. In the following, we will focus specifically on large scale layers. They are defined by a stratification anomaly greater than 1.5 and by an extension in isopycnal coordinates larger than $1/3^{\circ}$ (two adjacent stations) at the equator.

[9] As for the layers' zonal extent, the only zonal transect available along the equator (R/V Seward Johnson, summer 1997, courtesy Garzoli and Schmidt), indicates values up to 8° in isopycnal coordinates and thus reveals a strong anisotropy: we shall suppose throughout this paper that zonal variations are small compared to meridional ones.

3. Possible Mechanisms

[10] At high latitudes, occurrence of fine- or meso-scale density layering is often explained by double-diffusion [Schmitt, 1994]: this is corroborated by adequate distributions of the so-called Turner angle, a function of the salt and temperature gradients that allows the identification of linearly unstable zones. Typical Atlantic Turner angle profiles within 3° of the equator (Figure 3a) displays values such that the flow is either stable (between -45° and 45°) or marginally unstable (close to -45° or 45°) to double diffusive instability, especially between 600 and 2000 m. This suggests that this mechanism is not responsible for the large-scale Atlantic deep layering. Let us furthermore mention that double diffusion is not able to generate extended layers in upper-layer Pacific interleaving, as shown fairly convincingly by Edwards and Richards [2004].

[11] The deformation of isopycnal surfaces by internal waves strain has been invoked by Dengler and Quadfasel [2002] to explain the vertically homogeneous density layers which they observed in individual CTD profiles in the equatorial Indian Ocean. In the Atlantic case however, the large spatial scales of density layers (2° latitude, 100 m height) require a generation mechanism necessarily influenced by Earth rotation, which is not the case for internal waves. Furthermore, d'Orgeville and Hua [2004] have shown that internal wave signals, trapped within the deep equatorial track, only reach weak amplitudes and small meridional extents in their numerical simulations. We have thus opted not to pursue further studies of such processes.

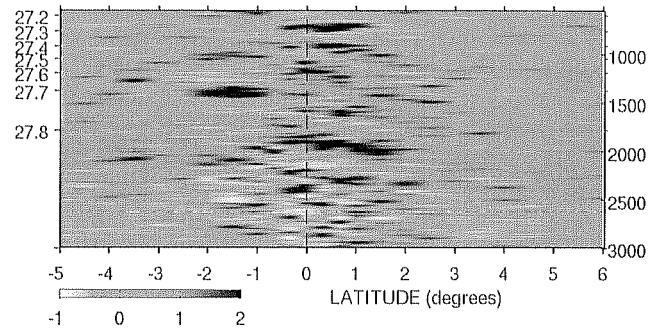


Figure 2. Stratification anomaly $(N^2 - \langle N^2 \rangle) / \langle N^2 \rangle$ at 23°W (EQUALANT 1999). Left axis: potential density ($\text{kg}\cdot\text{m}^{-3}$). Right axis: equivalent depth (m).

[12] A plausible mechanism that produces density layering is inertial instability, already invoked for the Pacific equatorial surface interleaving [Richards and Banks, 2002]. A flow is linearly inertially unstable as soon as: $fQ < 0$ [Hoskins, 1974] where f is the Coriolis parameter and Q is potential vorticity. This instability is most easily triggered in the immediate vicinity of the equator since f changes sign there. For equatorial phenomena whose zonal length scale is much larger than the meridional one, potential vorticity Q can be written in terms of angular momentum M as $Q \propto \partial_y M|_{\rho}$ (where y is the latitudinal distance from the equator and ρ is the density). We recall that for an equatorial β -plane, the angular momentum is defined as $M = U - \frac{1}{2}\beta y^2$ (where U is the local zonal velocity and β is the latitudinal variation of the Coriolis parameter f). For an unstable case, the $fQ < 0$ condition simply means that the maximum of angular momentum is displaced from the geographical equator. In observations, the diagnostic of $\partial_y M|_{\rho}$ in isopycnal coordinates (Figure 3b) shows that the meridional maximum of angular momentum ($\partial_y M|_{\rho} = 0$ solid line) lies alternatively south or north of the equator, so that the whole water column is inertially unstable.

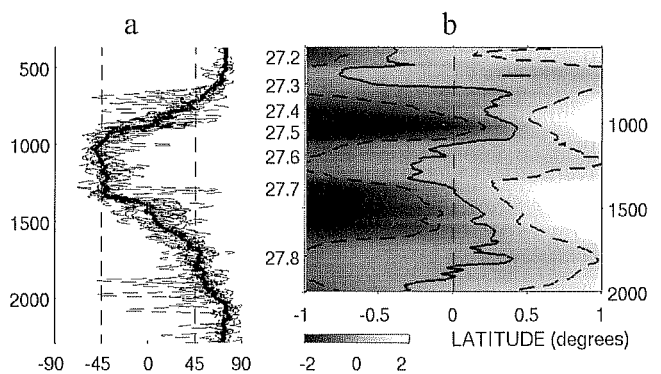


Figure 3. (a) Turner angle vertical profiles of stations between 3°S and 3°N at 23°W , with the thick solid line representing the mean. Within the $\pm 45^{\circ}$ vertical dashed lines, the flow is stable to double diffusion. (b) Section of $\partial_y M|_{\rho} \propto Q$ at 23°W between 1°S and 1°N . Left axis: potential density ($\text{kg}\cdot\text{m}^{-3}$). Right axis: equivalent depth (m). Color bar in 10^{-6}s^{-1} . Solid line: 0s^{-1} . Dashed lines: $\pm 10^{-6}\text{s}^{-1}$ (planetary vorticity at $y = \pm 0.4^{\circ}$). (EQUALANT 1999).

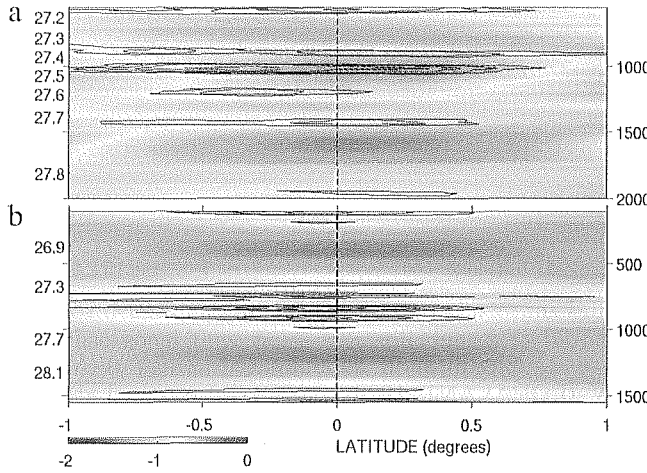


Figure 4. (a) Section at 10°W between 1°S and 1°N of the curvature $\partial_{yy}M|_\rho$. Left axis: potential density ($\text{kg}\cdot\text{m}^{-3}$). Right axis: equivalent depth (m). Colorbar in $\beta = 2.3 \cdot 10^{-11} \text{m}^{-1}\text{s}^{-1}$. Solid line: density jumps detected as explained in section 2. (EQUALANT 2000) (b) Same as (a) for our numerical simulation after non-linear saturation of the instability. Same filters as for observations (Appendix A) have been used.

[13] Nevertheless, this linear instability condition, already used in the western equatorial basin [Send *et al.*, 2002], cannot by itself justify the layering process. Further quantitative assessments identifying imprints of inertial instability are presented in the following section.

4. Support of Inertial Instability

4.1. Observations

[14] The inertial instability mechanism is a slanted convection process which is triggered to wipe out a maximum of angular momentum that is displaced from the equator.

[15] If we suppose that fluid parcels conserve their angular momentum M and density ρ , the nonlinear evolution of an inertially unstable zone leads to a meridional homogenization of M along isopycnal surfaces. Because of the y^2 dependence of the planetary contribution ($M = U - \frac{1}{2}\beta y^2$), due to Earth rotation, an assessment of both $\partial_y M|_\rho$ and curvature $\partial_{yy}M|_\rho$ is needed in order to detect meridional homogenization of M . (Note that $\partial_y M|_\rho$ is related to potential vorticity (section 3) and that $\partial_{yy}M|_\rho$ is related to the effective β -effect (section 4.2).) Latitudinal sections across the equator show that indeed $\partial_y M|_\rho \simeq 0$ for certain depth ranges (at 23°W , Figure 3b: grey values comprised between dashed lines), coinciding with westward jets. (The meridional structure of an equatorially centered jet is $U = U_0 + \frac{1}{2}\delta y^2 + o(y^2)$, with $\delta > 0$ (resp. < 0) for a westward (resp. eastward) jet. For a westward jet $|\partial_y M| \simeq |(\delta - \beta)y| < |\beta y|$ and $\partial_{yy}M \simeq \delta - \beta > -\beta$.) Curvature plots in isopycnal coordinate (at 10°W ; Figure 4a) highlight the same vertically localized zones where curvature is less than β in magnitude (yellow) and tends to 0 (red), meaning that the angular momentum M seems to be meridionally well-mixed on isopycnal surfaces there. But the outstanding result of Figure 4a is that density layering (black contours) mostly occurs within vertically-localized regions of homogeneous angular momentum (yellow and red) corresponding to westward jets.

[16] In the four EQUALANT transects of the western and central Atlantic basin [Bourlès *et al.*, 2003; Gouriou *et al.*, 2001], 23 layers have been detected between 600 and 2000 m depth: 90% are located where $-\beta < \partial_{yy}M|_\rho < 0$. This spatial correlation between layers and well-mixed angular momentum is further supported by the fact that the largest spatial coherency of layers coincides with the strongest homogenization in angular momentum as well as the strongest stratification anomalies: all the detected layers, that have an extension greater than 1° of latitude (4 stations), are located in parts of the flow where $-0.6\beta < \partial_{yy}M|_\rho < 0$ and have a stratification anomaly that can be greater than 2.5.

[17] Inertial instability is known to trigger meridional/vertical convective cells that meridionally redistribute angular momentum over large distances. Inside such extended cells, mixing of density leads to extended layering. Therefore the above spatial and strength correlations in in situ measurements confirm that inertial instability appears as the most plausible mechanism responsible for the extended equatorial density layering.

4.2. Numerical Simulations

[18] The equatorial zonal circulation presents large vertical scale westward/eastward equatorial deep jets (wave length of 500–800 m) within which the 50–100 m scale layering is embedded. The purpose of this section is to simulate numerically the smaller 50–100 m features in a two-dimensional model, while prescribing the deep jets background.

[19] We have performed very high resolution simulations with the model of Hua *et al.* [1997] (see Appendix B). A time-oscillating barotropic shear $\gamma(t)$, which is an idealization of the existing oceanic deep variability, forces the model and is able to induce inertial instability [d'Orgeville and Hua, 2004]. The prescription of the 800 m vertical scale jets background modulates further the strength of the instability. Indeed, westward jets ($U_{yy} < 0$) are much more propitious to inertial instability than eastward ones. Stevens [1983] explains this difference by a key parameter $\beta_n = \sqrt{\beta(\beta - U_{yy})}$ such that small values of β_n favours strong growth and large meridional extent of inertial instability.

[20] Numerical simulations reveal a large meridional coherency of density layering (Figure 5) with 70 m vertical scale. Such layering, obtained after a nonlinear saturation of the instability, displays the same localization as the observed one: Figure 4b, which presents in color the curvature $\partial_{yy}M|_\rho$ of the total angular momentum, displays extended layered structures (black contours) around the equator and located within zones of well-mixed angular momentum (westward jets, yellow and red). Moreover, the

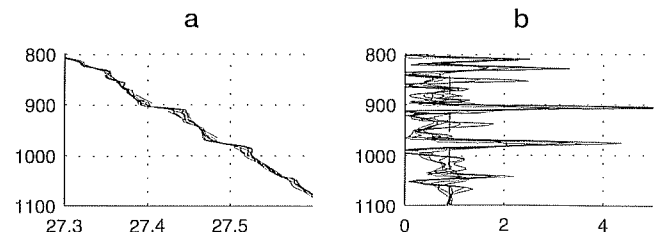


Figure 5. Same as Figure 1 but for our numerical simulation after nonlinear saturation of inertial instability.

latitudinal extent of layers increases when the background curvature $\partial_{yy}\bar{U}|_p \rightarrow \beta$.

5. Summary and Discussion

[21] We have presented possible in situ imprints of deep equatorial inertial instability at small vertical scales (50–100 m). Such processes are revealed by extended density layering which is spatially localized within regions of meridionally homogeneous angular momentum. Neither double diffusion nor internal waves strain are dynamically related to angular momentum unlike inertial instability. The latter thus appears as the most plausible explanation of our layering observations.

[22] Our interpretation is supported by numerical simulations of inertial instability which reproduce the main characteristics of the observations: extended layering, vertically localized within larger scale westward jets (regions of well-mixed angular momentum). A novel feature of the modelling is the inclusion of a barotropic time-oscillating shear to drive inertial instability which is vertically modulated by the prescription of steady baroclinic jets. Such idealized forcing is compatible with the long-lived character of the deep jets, that have a typical 500–800 m vertical scale in the Atlantic, compared to the high-frequency variability omnipresent throughout the whole water column (e.g., Bunge et al., submitted manuscript, 2004, and references therein).

[23] The time-oscillating nature of the forcing makes it possible to generate layering on both sides of the equator as in the observations, whereas applying a steady shear would lead to layers in a single hemisphere, which moreover have a narrower meridional extent. The vertical localization of the layering is identical for both types of forcing in the case where the baroclinic deep jets are prescribed.

[24] To explain the Pacific thermocline interleaving, Richards and Edwards [2003] invoke inertial instability in the upper layers due to the shear associated with the periodic displacement of the equatorial undercurrent (EUC). They model such mechanism by a steady latitudinal displacement of more than 1° of the EUC, thereby liberating the flow at the equator from the stabilizing effect of the strong eastward EUC curvature. At great depth, observed flows are substantially less energetic than in the thermocline and for realistic values of equatorial shear we suspect the curvature to play an important role for inertial instability.

[25] Besides mixing angular momentum, inertial instability also efficiently mixes all tracers. Oxygen and other tracers are meridionally well-mixed within westward jets (B. Bourlès and G. Charria, personal communication) for Intermediate Water masses. We have found stair-like structures in oxygen with the same localization and meridional/vertical scale as density. Inertial instability could thus be a candidate for the observed need for elevated mixing levels below the thermocline in equatorial areas, since the layering phenomenon is ubiquitous in all available equatorial transects throughout the subthermocline equatorial water column.

Appendix A: Data

[26] EQUALANT data used in this study are described by Gouriou et al. [2001] and Bourlès et al. [2003].

A1. Turner Angle

[27] Potential temperature θ and salinity S profiles are smoothed with a 30 m Hanning filter on a 1 m vertical grid. Turner angle profiles are then computed as $T_u = \arctan(\alpha^0 \partial_z \theta - \beta^S \partial_z S, \alpha^0 \partial_z \theta + \beta^S \partial_z S)$, where α^0 and β^S are local thermal expansion and saline contraction coefficients.

A2. Stratification Anomaly

[28] The Brunt-Väisälä frequency N is computed on a 5 m vertical grid for each station and N^2 -profiles are then smoothed vertically with a 100 m Hanning filter. For each section the mean profile $\langle N^2 \rangle$ is estimated by meridional averaging at each depth, in order to obtain the stratification anomaly profile $(N^2 - \langle N^2 \rangle) / \langle N^2 \rangle$ at each station. Those profiles are then interpolated on an isopycnal grid (Figures 2 and 4a).

A3. Shear and Curvature

[29] Zonal velocity is interpolated on the same isopycnal grid. For each section, an n -degree polynomial (where $2n$ is the number of stations) is computed to fit U in a least-squares sense at each density level and is used to calculate $\partial_y M|_p$ and $\partial_{yy} M|_p$ (Figures 3b and 4a, respectively).

Appendix B: Numerical Simulations

[30] Numerical simulations of section 4.2 use the zonally symmetric model of Hua et al. [1997]. Equations of motion are those of zonal velocity perturbation u , zonal vorticity $\xi = \nabla^2 \psi$ and total density $\rho = \bar{\rho} + \rho'$:

$$\begin{aligned} u_t + J(\psi, u) + (\beta y - \gamma(t) - \bar{U}_y) \psi_z + \bar{U}_z \psi_y &= \nu u_{zz} + \kappa u_{yy} \\ \xi_t + J(\psi, \xi) - \beta y u_z &= g \rho'_y / \rho_0 + \nu \xi_{zz} + \kappa \xi_{yy} \\ \rho_t + J(\psi, \rho) &= \nu \rho'_{zz} + \kappa \rho'_{yy} \end{aligned}$$

where J is the Jacobian operator $J(A, B) = A_y B_z - A_z B_y$. The above equations are integrated with vertical periodic conditions and a small initial random noise. Diffusion/dissipation coefficients are $\nu = 10^{-6} \text{ m}^2 \text{ s}^{-1}$ and $\kappa = 100 \text{ m}^2 \text{ s}^{-1}$.

[31] The barotropic time-oscillating shear is $\gamma(t) = \gamma_0 \cos(\omega_0 t)$ with $\gamma_0 = 1.4 \cdot 10^{-6} \text{ s}^{-1}$ and $\omega_0 = 4.6 \cdot 10^{-7} \text{ s}^{-1}$. The baroclinic steady shear corresponding to the deep jets is $\bar{U}(y, z) = (ay^4 + by^2 + c) \exp(-0.5(y/\lambda)^2) \cos(2\pi z/H)$ where $H = 800 \text{ m}$, $a = 1.1 \cdot 10^{-22} \text{ m}^{-3} \text{ s}^{-1}$, $b = -3.8 \cdot 10^{-12} \text{ m}^{-1} \text{ s}^{-1}$, $c = -0.25 \text{ ms}^{-1}$ and $\lambda = 1.4 \cdot 10^4 \text{ m}$. This baroclinic shear flow is in thermal wind balance with $\bar{\rho}(y, z)$. The mean Brunt-Väisälä frequency is $\langle N \rangle = 3.10^{-3} \text{ s}^{-1}$.

[32] **Acknowledgment.** The authors would like to thank Drs. F. Marin and M. Arhan for valuable comments on this work.

References

- Bourlès, B., et al. (2003), The deep currents in the eastern equatorial Atlantic Ocean, *Geophys. Res. Lett.*, 30(5), 8002, doi:10.1029/2002GL015095.
 Dengler, M., and D. Quadfasel (2002), Equatorial deep jets and abyssal mixing in the Indian Ocean, *J. Phys. Oceanogr.*, 32, 1165–1180.
 d'Orgeville, M., and B. L. Hua (2004), Equatorial inertial parametric instability of zonally symmetric oscillating shear flows, *J. Fluid. Mech.*, in press.
 Dunkerton, T. J. (1981), On the inertial stability of the equatorial middle atmosphere, *J. Atmos. Sci.*, 38, 2354–2364.

- Edwards, N. R., and K. J. Richards (2004), Nonlinear double-diffusive intrusions at the equator, *J. Mar. Res.*, *62*, 233–259.
- Gouriou, Y., et al. (2001), Deep circulation in the equatorial Atlantic Ocean, *Geophys. Res. Lett.*, *28*, 819–822.
- Hoskins, B. J. (1974), The role of potential vorticity in symmetric stability and instability, *Q. J. R. Meteorol. Soc.*, *100*, 480–482.
- Hua, B. L., D. W. Moore, and S. Le Gentil (1997), Inertial nonlinear equilibration of equatorial flows, *J. Fluid Mech.*, *331*, 345–371.
- Richards, K. J., and H. Banks (2002), Characteristics of interleaving in the western equatorial Pacific, *J. Geophys. Res.*, *107*(C12), 3231, doi:10.1029/2001JC000971.
- Richards, K. J., and N. R. Edwards (2003), Lateral mixing in the equatorial Pacific: The importance of inertial instability, *Geophys. Res. Lett.*, *30*(17), 1888, doi:10.1029/2003GL017768.
- Schmitt, R. W. (1994), Double diffusion in oceanography, *Annu. Rev. Fluid Mech.*, *26*, 255–285.
- Send, U., C. Eden, and F. Schott (2002), Atlantic equatorial deep jets: Space-time structure and cross-equatorial fluxes, *J. Phys. Oceanogr.*, *32*, 891–902.
- Stevens, D. (1983), On symmetric stability and instability of zonal mean flows near the equator, *J. Atmos. Sci.*, *40*, 882–893.

M. d'Orgeville, B. L. Hua, and R. Schopp, LPO, IFREMER, BP 70, F-29280 Plouzané, France. (marc.dorgeville@ifremer.fr; lien@ifremer.fr; richard.schopp@ifremer.fr)

L. Bunge, LODYC, IRD, Tour 45-55, 5ème étage, boîte 100, 4 Place Jussieu, F75252 Paris Cedex 05, France. (lbulod@lodyc.jussieu.fr)